Promoting Myelin Repair through In Vivo Neuroblast Reprogramming

Pascale Durbec, Myriam Cayre, Bilal El Waly

Stem Cell Reports
Article

ISSCR

OPEN ACCESS

Promoting Myelin Repair through *In Vivo* Neuroblast Reprogramming

Bilal El Waly,[1] Myriam Cayre,[1] and Pascale Durbec[1,*]
[1]1-Aix Marseille University, CNRS, IBDM-UMR 7288, Case 907, Parc Scientifique de Luminy, campus de Luminy, 13288 Marseille, Cedex 09, France
*Correspondence: pascale.durbec@univ-amu.fr
https://doi.org/10.1016/j.stemcr.2018.02.015

SUMMARY

Demyelination is frequently observed in a variety of CNS insults and neurodegenerative diseases. In rodents, adult neural stem cells can generate oligodendrocytes and participate to myelin repair. However, these cells mainly produce migratory neuroblasts that differentiate in the olfactory bulb. Here, we show that, in the demyelination context, a small subset of these neuroblasts can spontaneously convert into myelinating oligodendrocytes. Furthermore, we demonstrate that the contribution of neuroblasts to myelin repair can be improved by *in vivo* forced expression of two transcription factors: OLIG2 and SOX10. These factors promote directed fate conversion of endogenous subventricular zone neuroblasts into mature functional oligodendrocytes, leading to enhanced remyelination in a cuprizone-induced mouse model of demyelination. These findings highlight the unexpected plasticity of committed neuroblasts and provide proof of concept that they could be targeted for the treatment of demyelinated lesions in the adult brain.

INTRODUCTION

Oligodendrocyte loss and demyelination following CNS insults or neurodegenerative diseases lead to axonal suffering and impaired brain function. Spontaneous remyelination can occur, but this repair process is not always efficient, possibly due to the exhaustion of oligodendrocyte progenitor cells (OPCs) present in the brain parenchyma or to blockage in their maturation (Franklin, 2002). Studies in mouse models of demyelination have for a long time identified adult parenchymal OPCs as key actors of this repair process (Franklin et al., 1997). Interestingly, recent studies have demonstrated the unanticipated contribution of neural stem cells of the subventricular zone (SVZ) to myelin repair in rodent (Xing et al., 2014; Brousse et al., 2015). These cells display long-term self-renewal potential and, despite their restricted location, generate long-distance migrating progenitors that can contribute to myelin repair. During early post-natal stages, SVZ stem cells produce large amounts of OPCs that migrate into the surrounding structures (white matter, cortex [Cx], and striatum), and the majority of them eventually produces new oligodendrocytes (Suzuki and Goldman, 2003; Menn et al., 2006). The number of OPCs and oligodendrocytes produced by the SVZ drastically drops within 3–4 weeks following birth, and is then maintained at low levels throughout life (Capilla-Gonzalez et al., 2013). In case of a demyelinating insult, SVZ actively responds to demyelination by increasing the production of OPCs that will emigrate from the niche and form new myelinating oligodendrocytes (Menn et al., 2006).

In addition to OPCs, adult SVZ stem cells produce a large number of neuroblasts that perform long-distance migration through the rostral migratory stream (RMS) and become olfactory bulb (OB) interneurons (Lois and Alvarez-Buylla, 1994; Lois et al., 1996). Interestingly, in various degenerative or traumatic brain lesions, this population displays new migratory properties and invades various regions of the brain parenchyma (for review see Cayre et al., 2009). In particular, after demyelination, some SVZ neuroblasts are derouted from the RMS and ectopically migrate toward demyelinated sites (Nait-Oumesmar et al., 1999, 2007; Picard-Riera et al., 2002; Cantarella et al., 2007; Magalon et al., 2007; Goings et al., 2008; Cayre et al., 2013; Capilla-Gonzalez et al., 2014), where they spontaneously change their fate to produce myelinating oligodendrocytes (Jablonska et al., 2010). Likewise, SVZ neuroblasts grafted in dysmyelinated Shiverer mice perform long-distance migration along the white matter fiber tracts and efficiently produce oligodendrocytes (Cayre et al., 2006). Given the large number and high migration potential of SVZ neuroblasts, forcing this endogenous cell population to adopt an oligodendroglial fate could represent an interesting strategy to improve myelin repair in pathological conditions. In this context, in human brain, despite the presence of a neurogenic niche in the SVZ, the number of migratory neuroblasts is reduced in physiological conditions. Interestingly in multiple sclerosis (MS), SVZ has been shown to be reactivated and the number of neuroblasts increased; some of these neuroblasts co-expressed oligodendroglial markers (Nait-Oumesmar et al., 2007), highlighting their possible contribution to the repair process. Altogether, forcing endogenous cell population to adopt an oligodendroglial fate could represent an interesting strategy to improve myelin repair in pathological conditions.

OLIG2 and SOX10 are two key transcription factors involved in specification and differentiation of the oligodendroglial lineage (for review see El Waly et al., 2014; Mitew et al., 2014). OLIG2 is the only factor absolutely

required for OPC production. During development, *Olig2* inactivation leads to a reduced production of OPCs in most CNS regions (Lu et al., 2002; Zhou and Anderson, 2002), while SOX10 loss has no effect during determination but results in failure in terminal cell differentiation (Stolt et al., 2002). Recent studies have demonstrated that co-expressing OLIG2 and SOX10 in fibroblasts is sufficient to directly reprogram these cells into oligodendrocytes *in vitro* (Najm et al., 2013; Yang et al., 2013). Here we show that forcing expression of these two genes in SVZ neuroblasts induces their reprogramming into oligodendrocytes both *in vitro* and *in vivo*. This fate conversion is effective in both neonate and young adult brains and generates mature oligodendrocytes that form functional myelin. We further demonstrate that this forced reprogramming significantly enhances myelin repair in the adult brain after acute cuprizone-induced demyelination. These findings highlight the potential of targeting neuroblasts derived from the adult neurogenic niche to promote myelin repair.

RESULTS

Forced Expression of OLIG2 and SOX10 Converts SVZ-Derived Neuroblasts into Oligodendrocyte Progenitors in Cell Culture

We first tested whether forcing OLIG2 and/or SOX10 expression into SVZ neuroblasts could induce their reprogramming into oligodendrocytes *in vitro*. To do so, we co-electroporated neonate mouse brains with plasmids driving specific expression of these two factors (alone or in combination) specifically into SVZ neuroblasts using *Dcx* promoter (p*Dcx-Olig2*-IRES-*Cre*, p*Dcx-Sox10*-IRES-*Cre*, p*Dcx-Cre* for control), as well as plasmid driving strong and permanent GFP expression in the presence of CRE recombinase (pCMV-stopflox-m*Gfp*) (Figures 1A and S1). SVZs were dissected 1 day after electroporation, and cells were maintained in culture under differentiating conditions up to 7 days *in vitro* (DIV) (Figure 1A). When only control plasmid (CTL) was electroporated, no OLIG2$^+$ cells were observed among GFP$^+$ cells after 3 and 7 DIV (Figure 1B), showing that SVZ-derived neuroblasts do not spontaneously convert into oligodendrocytes *in vitro*. By contrast, after electroporation with *Olig2* (O) or *Sox10* (S) plasmids, around 70% of GFP$^+$ cells expressed OLIG2 (Figure 1B). Interestingly, the proportion of GFP$^+$OLIG2$^+$ cells was significantly higher when *Olig2* and *Sox10* were co-electroporated (Figure 1B), indicating a cooperative effect of these two factors.

To further analyze the ability of OLIG2 and SOX10 to initiate SVZ neuroblast reprogramming, we then tested whether their forced expression induces endogenous OLIG2/SOX10 expression. We performed qRT-PCR to monitor *Olig2* and *Sox10* exogenous and total transcript levels (exogenous plus endogenous, see the Experimental Procedures) in electroporated cells over time (Figures S2A–S2D). In cells electroporated with control plasmids, exogenous *Olig2* and *Sox10* transcripts were undetectable, while total transcripts levels remained low and unchanged over time (data not shown). In cells co-electroporated with *Olig2* and *Sox10* (SO), exogenous transcripts levels increased until 3 (*Olig2*) and 4 DIV (*Sox10*), and then progressively decreased until 6 DIV (Figures S2A and S2C). In the meantime, *Olig2* and *Sox10* total transcripts levels continuously increased until 6 DIV (Figures S2B and S2D), indicating that endogenous expression of these factors took over their forced expression. In agreement, we observed a significant decrease in the proportion of GFP$^+$ cells expressing DCX between 3 and 7 DIV (from 41% ± 3.7% to 31% ± 2.2%; $p = 0.047$). Thus, forcing expression of OLIG2 and SOX10 into SVZ neuroblasts induces expression of endogenous transcription factors sufficient to commit these cells to the oligodendrocyte lineage.

We next analyzed the morphology and branching complexity of *Olig2/Sox10* co-electroporated cells after 3 and 7 DIV (Figures 1C–1E; see Experimental Procedures and Figures S2E and S2F). Newborn neuroblasts in post-natal brain are migrating cells with mono- or bipolar morphology, and DCX has been shown to be essential in maintaining such morphology (Koizumi et al., 2006). By contrast, immature oligodendrocytes display a high number of processes and branching (Trapp et al., 1997). As expected, control DCX$^+$GFP$^-$ neuroblasts were bipolar, with low branching complexity, and did not express OLIG2. On the contrary, control OLIG2$^+$GFP$^-$ oligodendroglial cells were multipolar, with high branching complexity, and did not express DCX (Figures S2E and S2F). Interestingly, GFP$^+$OLIG2$^+$ electroporated cells could be classified into three categories exhibiting morphologies and branching complexities intermediate between neuroblasts and oligodendrocytes (Figure 1C): (1) DCX$^+$ bipolar cells with low branching complexity, (2) DCX$^-$ bipolar cells with low branching complexity, and (3) DCX$^-$ multipolar cells with typical oligodendroglial multipolar morphology and high branching complexity. The synergic effect of SOX10 and OLIG2 was again observed in the distribution of GFP$^+$OLIG2$^+$ cells within the three categories, at 3 DIV: the combination of the two factors induced a shift toward category 3 (Figure 1D). Beside, after SO electroporation the percentage of category 1 cells resembling neuroblasts decreased over time (Figure 1E, 29% at 3 DIV versus 21% at 7 DIV; $p = 0.028$, $N = 255$) while category 3 resembling oligodendrocytes increased (Figure 1E, 42% at 3 DIV versus 53% at 7 DIV; $p = 0.008$, $N = 488$). These results therefore suggest that electroporated neuroblasts change shape and acquire an oligodendroglial morphology over time through a continuum of intermediate states.

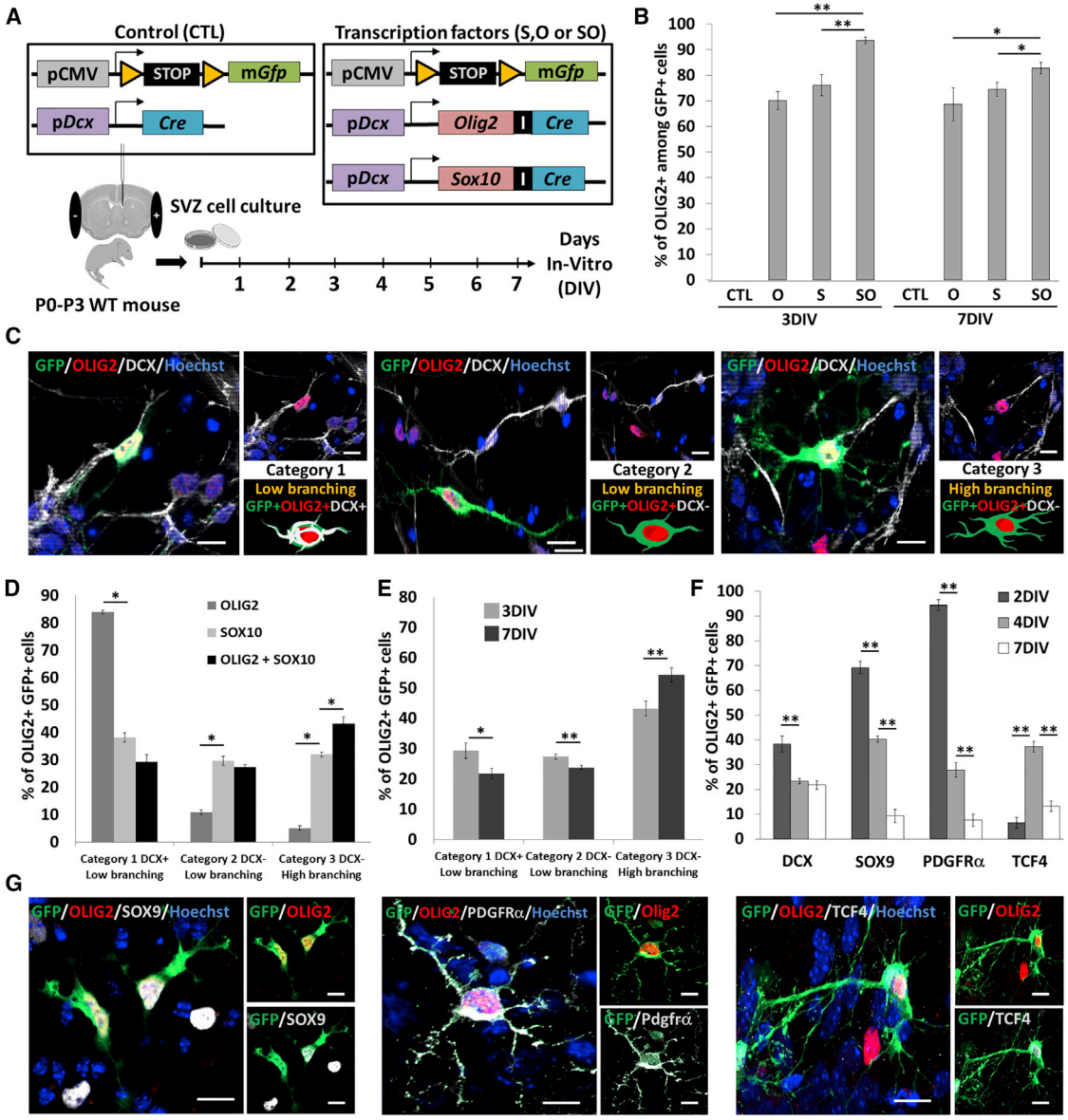

Figure 1. Transdifferentiation from Neuroblasts to Oligodendrocytes *In Vitro* by Forced Expression of SOX10 and/or OLIG2

(A) Schematic description of the constructs and experimental design to force the expression of OLIG2 (O) and/or SOX10 (S) in SVZ neuroblasts. Newborn mice were electroporated with either control plasmids (CTL), or transcription factors plasmids, alone or associated (SO).

(B) Graphs showing the percentage of $OLIG2^+$ cells among GFP^+ cells after 3 and 7 DIV (n = 5). Expression of both SOX10 and OLIG2 significantly increases the percentage of $OLIG2^+$ cells compared with control or each factor alone.

(C) Representative images of the three categories of GFP^+OLIG2^+ cells after 3 DIV classified on the basis of cell morphology (low and high branching) and DCX expression.

(D) Distribution of GFP^+OLIG2^+ cells within the three categories, at 3 DIV, after expression of OLIG2, SOX10, or both (n = 5).

(E) Distribution of GFP^+OLIG2^+ cells within the three categories, at 3 and 7 DIV, after expression of SOX10 and OLIG2 together (n = 5).

(F) Phenotypic characterization of GFP^+OLIG2^+ cells after 2, 4, and 7 DIV, using DCX, (neuroblast marker), SOX9 (OPC marker), PDGFRα (OPC and pre-oligodendrocyte marker), and TCF4 (pre-oligodendrocyte marker) (n = 3 experiments).

(G) Illustrations of SOX9, PDGFRα, and TCF4 expression in GFP^+OLIG2^+ cells at 4 DIV after forced expression of both SOX10 and OLIG2.

Error bars represent mean ± SEM. Scale bars represent 10 μm. *p < 0.05, **p < 0.01; Mann-Whitney test. P0–P3, post-natal days 0–3. See also Figure 2.

To confirm this fate change we monitored expression of neuronal and oligodendroglial lineage markers in cultured electroporated cells after 2, 4, and 7 DIV (Figures 1F and 1G). We showed that, while in control condition all GFP$^+$ cells expressed DCX (Figures S3A–S3C, 100% n = 5 independent experiments), forced SO expression led to a strong reduction of this marker (Figure 1F); SOX9 and PDGFRα (oligodendrocyte progenitor markers) are expressed by GFP$^+$OLIG2$^+$ cells as early as 2 DIV suggesting rapid initiation of fate conversion of neuroblasts. These two OPC markers significantly decreased until 7 DIV, while the percentage of GFP$^+$OLIG2$^+$ cells expressing TCF4 (a pre-oligodendrocyte marker) transiently increased, suggesting a maturation of these cells along the oligodendroglial lineage.

Altogether, these findings demonstrate that forcing expression of OLIG2 and SOX10 into SVZ neuroblasts *in vitro,* induces their reprogramming into oligodendrocyte lineage cells.

Forced OLIG2 and SOX10 Expression *In Vivo* during Developmental Myelination Period Changes the Migration Behavior of SVZ-Derived Neuroblasts and Converts Them into Myelinating Oligodendrocytes

To analyze the differentiation potential of transfected neuroblasts *in vivo*, we electroporated neonate mouse SVZ with *Olig2/Sox10* and characterized transfected cells over a 6-week period, corresponding to an intense phase of oligodendrocyte terminal differentiation and myelin formation starting from the striatum and the corpus callosum (CC) (Dai et al., 2015).

In these experiments, we took advantage of the mT/mG mouse line, in which CRE-induced recombination triggers expression of myristoylated GFP, a GFP variant targeted to the membrane that allows visualization of myelin segments. mT/mG pups were electroporated with p*Dcx-Olig2*-IRES-*Cre* and p*Dcx-Sox10*-IRES-*Cre* (SO) or with control p*Dcx-Cre* (CTL) plasmids (Figure 2A). Two days post-electroporation (dpe), we observed 48.7% ± 8.9% (n = 3) GFP$^+$ cells among DCX$^+$ neuroblasts in the SVZ (Figure S3D). Conversely, virtually all GFP$^+$ cells in the SVZ were DCX$^+$ (Figure S3D). At this early time point (2 dpe), 90% ± 1.7% of GFP$^+$ cells co-express OLIG2, validating our electroporation strategy to force transcription factor expression in SVZ neuroblasts (Figure S3E). As expected, in control conditions, the vast majority of GFP$^+$ cells (neuroblasts) was located in the SVZ and RMS/OB with clear predominance in the RMS/OB after 5 dpe (Figures 2C and S4). By contrast, in SO electroporated brains, GFP$^+$ cells were observed in SVZ surrounding structures, first in the striatum (5 dpe) and later in the CC and cortex (Cx) (14 and 42 dpe) (Figures 2B and 2C). Strikingly, at 42 dpe only a minority (9% ± 2%) of GFP$^+$ cells remained in the RMS/OB. The majority of these cells was instead found in the CC/Cx (51% ± 2%) and the striatum (24% ± 3%) (Figures 2B, 2C, and S4). These results demonstrate that co-expression of OLIG2 and SOX10 in SVZ neuroblasts changes their migratory behavior and favors their emigration from the SVZ/RMS toward adjacent structures, in a process reminiscent of SVZ-derived OPC behavior in normal conditions in neonate brain (Suzuki and Goldman, 2003).

We next analyzed the fate of GFP$^+$ cells present in the CC, Cx, and striatum 42 days after forced SOX10/OLIG2 expression (Figures 2D and 2E; Table 1). We observed no DCX$^+$ cells but the majority of GFP$^+$ cells were committed to the oligodendroglial lineage and were differentiated as mature CC1$^+$ oligodendrocytes (Figures 2D and 2E; Table 1). They displayed a typical shape of myelinating oligodendrocytes with GFP$^+$/MBP$^+$ long segments (Figure 2F) decorated with CASPR/PARANODIN (Figure 2G), suggesting that myelin segments with functional nodes of Ranvier. Besides, a fraction of GFP$^+$ cells retained an astrocytic phenotype and expressed GFAP (Table 1). Altogether these results demonstrate that forced expression of OLIG2 and SOX10 in post-natal brain transdifferentiates SVZ-derived neuroblasts into mature, myelinating oligodendrocytes in surrounding white and gray matter structures.

Fate Conversion of Neuroblasts into Myelinating Oligodendrocytes Is Effective in Young Adult Brain

A few weeks after birth, oligodendrogenesis is decreased and the production of new oligodendrocytes from the SVZ is very low compared with neuron production. To determine whether neuroblast transdifferentiation is still possible in this context, we designed new plasmids expressing an inducible CRE (*CreERT2*) under the control of *Dcx* promoter (Figure 3A). Electroporation was performed in neonate mT/mG mice and CRE recombination was induced by tamoxifen intraperitoneal injections in 5-week-old mice. The effectiveness of this protocol was validated (see Figures S3F and S3G). This strategy triggers expression of SOX10 and OLIG2 (SO) in migratory neuroblasts in the SVZ and the RMS without using invasive procedures that could interfere with SVZ homeostasis. In control conditions 14 and 42 days after tamoxifen injection, all GFP$^+$ cells were located in the SVZ/RMS/OB system (enrichment in RMS/OB) (Figure 3C). By contrast, in OLIG2/SOX10 electroporated brains, tamoxifen injection led to ectopic migration of nearly 30% of GFP$^+$ cells in surrounding structures at both 14 dpi (Figures 3B and 3C) and 42 dpi (Figure 3C), with equivalent proportions in the striatum and the CC/Cx. At 42 dpi, the majority of GFP$^+$ cells present outside the SVZ/RMS/OB pathway had differentiated into mature oligodendrocytes expressing CC1 (Figure 3D; Table 1). In the CC, GFP$^+$CC1$^+$ oligodendrocytes represented up to 3% ± 1% of all CC1$^+$ cells. These GFP$^+$ cells displayed typical morphology of ramified oligodendrocytes

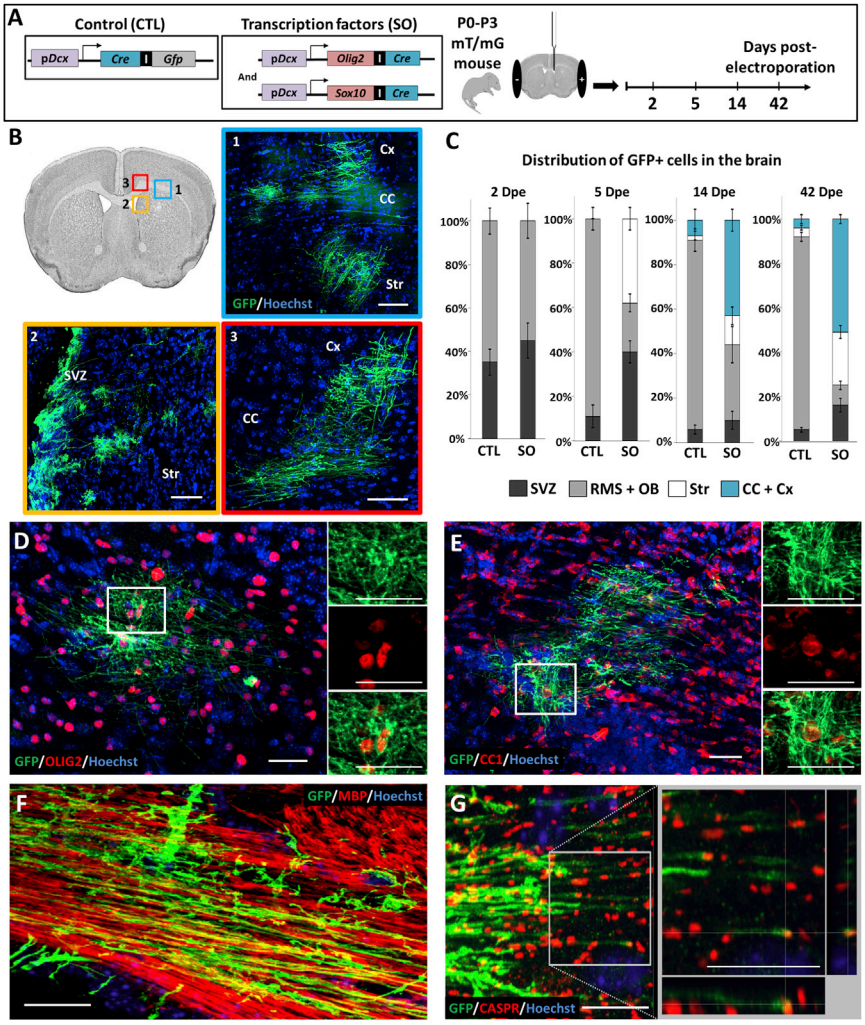

Figure 2. *In Vivo* Neuroblast to Oligodendrocyte Transdifferentiation in the Neonate Brain by Forced Expression of SOX10 and OLIG2

(A) Schematic description of the constructs and experimental design to force the expression of SOX10 and OLIG2 (SO) in SVZ neuroblasts by electroporation in neonate mT/mG mice.

(B) Forty-two days post-electroporation (dpe) GFP$^+$ cells are observed in, striatum (1), SVZ (2), and CC and Cx (3).

(C) Distribution of GFP$^+$ cells in different brain structures at 2, 5, 14, and 42 dpe in control or SO condition (n = 8 mice per group). Error bars represent mean ± SEM. Except at 2 dpe, the differences in GFP$^+$ cell distribution between CTL and SO groups are significant with $p < 0.001$.

(D–F) Immunolabeling against OLIG2, red in (D), CC1 for mature oligodendrocyte, red in (E), and MBP, red in (F), showing the oligodendroglial differentiation of GFP$^+$ cells 42 dpe.

(G) Immunolabeling showing the PARANODIN (CASPR) labeling at the tip of GFP$^+$ segments indicating the presence of a node/paranode organization. Note that in (D)–(G), OLIG2, MBP, CC1, and CASPR shown in red in the pictures were labeled with an Alexa 567 secondary antibody to avoid overlap with tomato signal from mT/mG mice.

Scale bars represent 20 μm. Cx, cortex; Str, striatum.

(Figures 3D–3F). They extend long and straight MBP-expressing myelin segments that co-localize with CASPR/PARANODIN at the level of axoglial junctions in the nodes of Ranvier (Figures 3E and 3F). SVZ-derived astrocytes, which were undetectable in control conditions, were found in insignificant proportion in *Olig2/Sox10* electroporated brains (Table 1). Altogether, these results demonstrate that SVZ-derived neuroblasts produced during adulthood remain competent to transdifferentiate and do migrate efficiently in the mature brain to produce new myelinating oligodendrocytes in the striatum, CC, and Cx.

Fate Conversion of SVZ-Derived Neuroblasts Improves Remyelination in the Adult Brain

To determine whether transdifferentiated neuroblasts could participate and eventually favor myelin repair, we exposed *Sox10/Olig2* electroporated mice to cuprizone-induced demyelination (Figure 4A). Electroporation was performed in neonates and 5 weeks after, mice were fed with cuprizone for 5 weeks to induce demyelination. In the second week of cuprizone treatment, SOX10 and OLIG2 expression was induced in SVZ-derived neuroblasts by tamoxifen injection, initiating their fate conversion (Figure 4A). The efficiency of cuprizone-induced demyelination did not differ in CTL and SO groups, as demonstrated by the similar drop in OLIG2 and CC1$^+$ cell density after 3 weeks of cuprizone diet (Figure S5A) and by the similar density of myelinated axons in the CC assessed by electron microscopy at the peak of demyelination (Figure S5B). Thus forced SO expression during cuprizone treatment did not protect from demyelination.

Distribution of GFP$^+$ cells and their contribution to myelin repair was analyzed 2 weeks after cuprizone removal in the CC, which is one of the most demyelinated structures in this model. In contrast to our previous experiments performed in non-injured context, we observed that cuprizone-dependent demyelination induced a clear

Table 1. Phenotype of Transfected Cells in Periventricular Brain Structures 42 Days after the Induction of OLIG2 and SOX10 Expression

		Condition	GFP$^+$ OLIG2$^+$ (%)	GFP$^+$ OLIG2$^+$CC1$^+$ (%)	GFP$^+$ GFAP$^+$ (%)	GFP$^+$ DCX$^+$ (%)
Neonate brain	CC and Cx	CTL	0	0	91 ± 8	0
		SO	89 ± 5	85 ± 7	8 ± 4	0
	Striatum	CTL	0	0	75 ± 19	0
		SO	61 ± 8	53 ± 11	15 ± 6	0
Healthy adult brain	CC and Cx	CTL	NA	NA	NA	NA
		SO	82 ± 10	64 ± 8	14 ± 6	0
	Striatum	CTL	NA	NA	NA	NA
		SO	58 ± 2	52 ± 3	19 ± 5	0

Transfected GFP$^+$ cells present in corpus callosum, cortex, and striatum were phenotyped using oligodendrocytic and astrocytic markers. NA, non-applicable (no cell).

emigration of GFP$^+$ cells from SVZ/RMS toward the CC when CTL plasmid was electroporated (Figures 4B and S4). This indicates that, after demyelination, neuroblasts are mobilized and spontaneously emigrate toward demyelinated CC. Strikingly, overexpression of SOX10 and OLIG2 induced a 3-fold increase of GFP$^+$ cell mobilization in the CC and Cx and a 2-fold increase in the striatum (Figures 4B and 4C). As expected, this was accompanied by a significant decrease of the number of GFP$^+$ cells present in the RMS/OB (from 205 ± 28.6 to 79.33 ± 9.84 in CTL and SO groups, respectively) (Figure 4B).

We checked that GFP$^+$ cells electroporated with *Sox10* and *Olig2* indeed produced myelinating oligodendrocytes in this pathological context. We observed GFP$^+$ segments ensheathing axons labeled with neurofilament (Figure 4D), and the tips of GFP$^+$ segments were decorated with CASPR (Figure 4D) and βIV-SPECTRIN labeling (Figure 4E) suggesting that GFP$^+$ cells produced functional myelin segments decorated by the nodes of Ranvier. Finally, electron microscopy coupled with GFP immunogold labeling unequivocally demonstrated that converted neuroblasts form compact myelin sheath around axons (Figure 4F).

To evaluate the contribution of electroporated cells to remyelination, we first quantified the area occupied by mGFP labeling in the CC as an indicator of GFP$^+$ myelin segments extension. We observed that the GFP$^+$ area in the demyelinated CC was 5-fold higher after SO than after CTL electroporation (Figure 4G). Furthermore, the quantification of pixels double-positive for GFP and MBP shows that 80.2% ± 6.9% of GFP$^+$ pixels in the CC are also MBP$^+$ (Figure 4G), suggesting that transdifferentiated SVZ neuroblasts actively participate in the remyelination process. We then estimated remyelination by quantifying the MBP$^+$ area in the CC (Figure 4H). As expected at this time point (2 weeks after cuprizone removal), CC remyelination was not yet complete (61.8% ± 1.4% MBP$^+$ area in CC of cuprizone-treated mice versus 92% ± 7.7% in control mice not fed cuprizone; $p = 0.003$). Interestingly SO electroporation in cuprizone-treated mice triggered a significant increase in MBP$^+$ area in the CC in the electroporated side compared with the contralateral side, and also compared with GFP electroporated mice (Figure 4H). To note, 14.5% ± 2.2% of MBP$^+$ pixels co-labeled with GFP in the SO electroporated side (Figure 4C) showing the contribution of electroporated cells to enhanced myelin repair. Thus, although full remyelination is known to spontaneously occur in the cuprizone model (usually 4 weeks after cuprizone removal), forced SO expression in neuroblasts can accelerate this repair process (Figure 4H). Strikingly, animals with extensive GFP labeling in the CC were those with highest CC myelination, highlighting a positive correlation between the GFP$^+$MBP$^+$ and MBP$^+$ areas in the CC, both in CTL and SO conditions, suggesting efficient contribution of SVZ-derived neuroblasts to the remyelination process (Figure 4I). It is important to note the clear shift toward more myelin coverage in the SO group (Figure 4I). Thus, forcing expression of SOX10 and OLIG2 in SVZ neuroblasts significantly improves the remyelination process.

Altogether these data show that endogenous SVZ neuroblasts spontaneously contribute to remyelination upon cuprizone treatment. They also demonstrate that forcing fate conversion of this cell population into myelinating oligodendrocytes significantly enhances this spontaneous regenerative process.

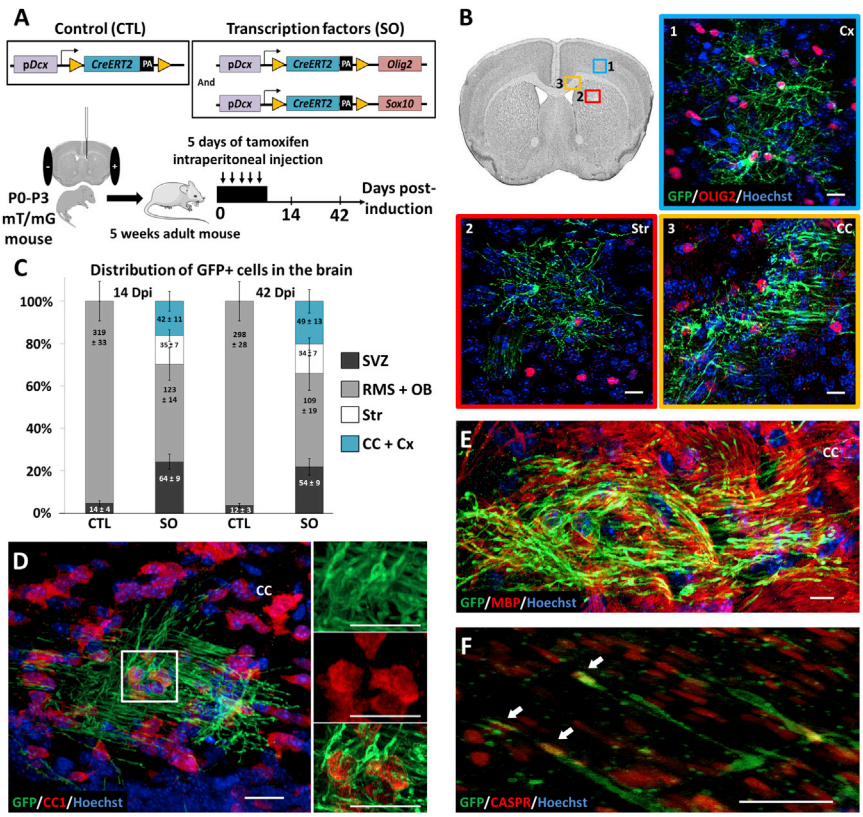

Figure 3. *In Vivo* Neuroblast to Oligodendrocyte Transdifferentiation in the Young Adult Brain by Forced Expression of SOX10 and OLIG2

(A) Schematic description of the constructs and experimental design to force the expression of SOX10 and OLIG2 (SO) in SVZ neuroblasts in young adult mT/mG mice. mT/mG pups are electroporated with plasmids (CTL or SO) driving inducible CRE expression, and transcription factor expression is induced in the adult mouse by tamoxifen injections.

(B) Fourteen days after the first tamoxifen injection in mouse electroporated with SO, GFP$^+$ cells are identified in periventricular structures.

(C) Histogram showing the distribution of electroporated cells in CTL or SO mouse brains at 14 and 42 days after the first tamoxifen injection (n = 9 mice per group). The differences between CTL and SO distribution at each stage are significant with $p < 0.001$ using the chi-square test. Error bars represent mean ± SEM.

(D–F) Immunolabeling 14 days after induction of SO expression, showing the oligodendroglial differentiation of GFP$^+$ cells based on the expression of CC1 (D), MBP (E), and of PARANODIN (CASPR) at the tip of GFP$^+$ segments (F) (white arrow). Note that in (B) and (D–F), OLIG2, MBP, CC1, and CASPR shown in red in the pictures were labeled with an Alexa 567 secondary antibody to avoid overlap with tomato signal from mT/mG mice.

Scale bars represent 20 μm. CC, corpus callosum; Cx, cortex; Str, striatum.

DISCUSSION

In rodent models of demyelination, both parenchymal OPC- and SVZ-derived progenitors have been shown to participate in spontaneous myelin repair (Xing et al., 2014; Brousse et al., 2015). Here we show that SVZ-derived neuroblasts also contribute to myelin repair via spontaneous fate reprograming into oligodendrocytes, and that such reprograming can be forced experimentally, accelerating remyelination. We demonstrate that forced expression, specifically in neuroblasts, of two key regulators of oligodendrogenesis (OLIG2 and SOX10) can efficiently turn on endogenous oligodendroglial genes and convert neuroblasts into oligodendrocytes. This fate conversion during myelin formation in neonates, and later in the juvenile brain, leads to the formation of myelinating oligodendrocytes in gray and white matter structures surrounding SVZ/RMS. We finally show that forced expression of these two transcription factors promotes myelin repair in a mouse model of demyelination.

OPC specification and differentiation are dynamic processes controlled by the expression of key regulators. The sustained expression of SOX10 and OLIG2 has been shown to induce reprogramming of various cell types toward oligodendrocytic fate (Najm et al., 2013; Yang et al., 2013). During oligodendrocyte development both genes have distinct functions: OLIG2 is instrumental for cell fate specification (Zhou et al., 2001), whereas SOX10 is necessary for cell differentiation and maturation, inducing key elements of the regulatory network of differentiating oligodendrocytes, including OLIG1, NKX2.2, and MYRF (Stolt et al., 2002; Weider et al., 2015). In agreement with this, the main cell population present in our culture after forced expression of OLIG2 was category 1 (GFP$^+$, OLIG2$^+$, DCX$^+$, and low branching), whereas after forced expression of SOX10 we observed more of categories 2 (GFP$^+$, OLIG2$^+$, DCX$^-$, and low branching) and 3 (GFP$^+$, OLIG2$^+$, DCX$^-$, and high branching) (Figure S3B). Furthermore, the combined expression of both factors produced synergistic effects compared with each factor alone. These results are consistent with reports showing that there are complex

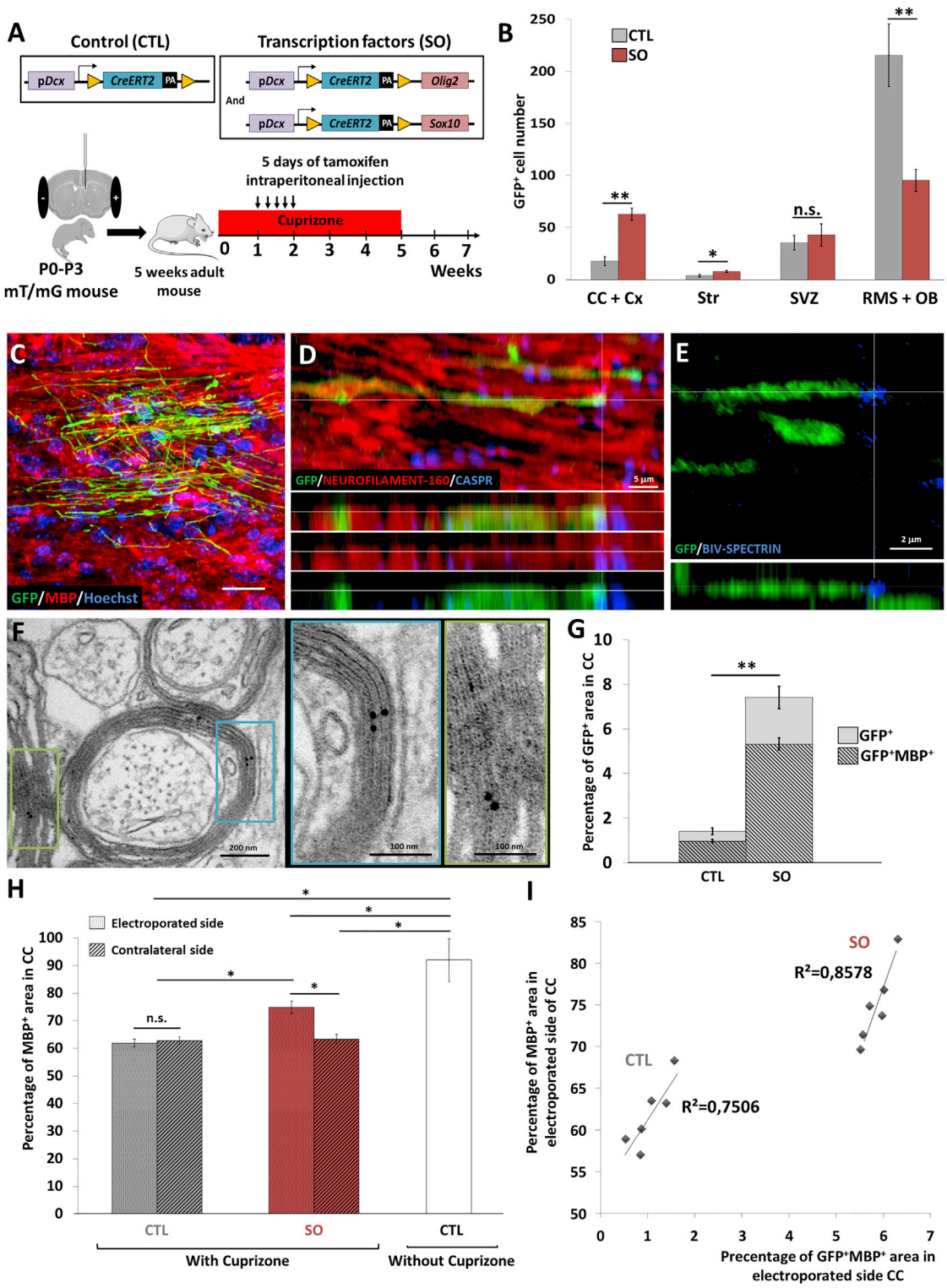

Figure 4. Forced Neuroblast to Oligodendrocyte Transdifferentiation Promotes Remyelination in the Cuprizone Mouse Model of Demyelination

(A) Schematic description of the constructs and experimental design to force the expression of SOX10 and OLIG2 (SO) in SVZ neuroblasts after cuprizone-induced demyelination, a mouse model of multiple sclerosis. mT/mG pups are electroporated with plasmids driving

(legend continued on next page)

reciprocal interactions between these two factors, OLIG2 activating SOX10 directly (Kuspert et al., 2011) and SOX10 modulating the expression of OLIG2 (Liu et al., 2007; Weider et al., 2015). This regulatory loop probably plays a key role in the regulation of the endogenous genetic program, allowing progression along the oligodendrocyte lineage in physiological conditions and during remyelination. Similar cooperation between SRY-related HMG-box and basic-helix-loop-helix transcription factors has been shown to be instrumental for cell fate conversion of glial progenitors into neurons in lesioned brain (Heinrich et al., 2014). Interestingly, our qPCR analysis (Figures S2A–S2D) demonstrates that, 3 days after electroporation, the transcription of exogenous OLIG2 and SOX10 decreases (in relation with the disappearance of DCX expression in transfected cells) and the endogenous program takes over. Any failure in the relay between exogenous and endogenous OLIG2 production could lead to astrocyte differentiation, as suggested by the study of Zhu et al. (2012) showing that OLIG2 deletion in NG2 cells triggers astrocyte production. We indeed observed few neuroblast-derived astrocytes in the CC after forced fate conversion indicating that reprogramming through forced expression of SOX10 and OLIG2 is efficient in the CC.

Conversion of differentiated cells into neuron *in vitro* or *in vivo* has been extensively studied (An et al., 2016). By contrast, the direct conversion of differentiated cells into oligodendrocytes has received less attention. Fibroblasts have been reprogramed *in vitro* and transplanted in animal models of demyelination to follow their terminal differentiation and contribution to myelin repair (Najm et al., 2013; Kim et al., 2015). Very few studies have considered the conversion of endogenous cells into oligodendrocytes *in vivo* (Marshall et al., 2005). Adult neural stem/progenitor cells have the potential to produce oligodendrocytes but physiologically mainly produce neurons. Forced expression of ASCL1, OLIG2, and SOX10 in dentate gyrus neural stem/progenitor cells allowed to push these cells into the oligodendrocytic lineage, and these newly formed oligodendrocytes then locally contributed to myelin repair after focal injury (Braun et al., 2015). Here, we moved a step further by targeting progenitors already committed to the neuronal fate. SVZ-derived neuroblasts are constantly produced in the adult brain in significant quantity and exhibit long-distance migratory behavior both in the RMS and in white matter fiber tracts after grafting (Cayre et al., 2006). Furthermore, after injury or demyelination, neuroblasts emigrate from the SVZ/RMS and scatter in surrounding structures (Cayre et al., 2009; Nait-Oumesmar et al., 2007). Although SVZ-derived neuroblasts have already adopted a neuronal fate, they seem to maintain a high plasticity potential since they are still able to change fate and form myelinating cells (Cayre et al., 2006; Jablonska et al., 2010). Our results demonstrate that SVZ-derived neuroblasts can spontaneously convert into oligodendrocytes after cuprizone-induced demyelination and contribute to remyelination; furthermore, this process can be boosted by forced expression of SOX10 and OLIG2. In this context, our results represent a proof of concept for the use of endogenous SVZ-derived neuroblasts to improve remyelination by forcing their transdifferentiation into myelinating oligodendrocytes. Previous studies have forced oligodendrocyte fate in neural stem cells either by genetic (Marshall et al., 2005) or pharmacological (Samanta et al.,

inducible CRE expression. Cuprizone feeding starts 5 weeks after electroporation for a 5-week period. Transcription factor expression is induced in the adult mouse by tamoxifen injections during the second week of cuprizone feeding.

(B) Distribution of GFP^+ cells in mouse brains 2 weeks after cuprizone removal, after either electroporation of control plasmid (CTL) or transcription factors plasmids (SO). More than 200 cells were counted per brain; n = 6 mice per condition. (*$p < 0.05$, **$p < 0.01$; Mann-Whitney test).

(C–E) Immunolabeling 2 weeks after stopping cuprizone treatment, showing the oligodendroglial differentiation of GFP^+ cells based on the expression of MBP (C). Scale bar in C represents 20 μm. NEUROFILAMENT-160 and PARANODIN (CASPR) (D) or βIV-SPECTRIN (E) labeling show that myelin segments enwrap axons and are terminated by the nodes of Ranvier.

(F) Electron micrograph showing GFP immunogold-labeled myelin sheath in the CC of mice electroporated with SOX10 and OLIG2. Note the presence of gold beads in compact myelin sheaths surrounding an axon, attesting the differentiation of electroporated neuroblasts into myelinating oligodendrocytes.

(G) Quantitative analysis of GFP^+ and GFP^+MBP^+ area percentage in the CC in the electroporated hemisphere in control (CT) and the SO condition (n = 6 mice per condition). **$p < 0.01$; Mann-Whitney test.

(H) Graph comparing the percentage of MBP^+ area in the CC between electroporated and contralateral hemispheres in CTL and SO conditions (n = 6 brains per condition) and in untreated control mice (no cuprizone). *$p < 0.05$; Wilcoxon paired test.

(I) Percentage of MBP^+ area positively correlates with the percentage of GFP^+MBP^+ area in the CC in CTL and SO conditions indicating the contribution of reprogramed neuroblasts to remyelination (n = 6 mice per condition). Error bars represent mean ± SEM. Note that in (C) and (D), MBP and NEUROFILAMENT-160 shown in red were labeled with an Alexa 567 secondary antibody to avoid overlap with tomato signal from mT/mG mice.

RMS, rostral migratory stream; OB, olfactory bulb; CC, corpus callosum; Cx, cortex; Str, striatum; SVZ, subventricular zone. See also Figure S5.

2015) manipulations; our strategy specifically targeting committed neuronal progenitors could present the advantage to avoid neural stem cell depletion preserving the neurogenic niche.

Adult neurogenesis exists in the human brain (Ernst and Frisen, 2015), but in physiological conditions neuroblast production is reduced. Interestingly in MS, SVZ is reactivated and the number of migrating neuroblasts increases, some of them co-expressing oligodendroglial markers (Nait-Oumesmar et al., 2007). This suggests that, in humans as in mice, SVZ-derived neuroblasts may transdifferentiate and represent a complementary source of cells for myelin repair in periventricular zones. The development of pharmacological tools to promote such cell fate change could be taken into consideration for future therapeutic strategies.

EXPERIMENTAL PROCEDURES

Animals, Treatments, Demyelination, and Electroporation

All experimental and surgical protocols were performed following the guidelines established by the French Ministry of Agriculture (Animal Rights Division). The architecture and functioning rules of our animal house, as well as our experimental procedures have been approved by the "Direction Départementale des Services Vétérinaires" and the ethic committee (ID numbers F1305521 and 2016071112151400 for animal house and research project, respectively).

Neonate CD1 wild-type mice (P0–P3) (from Janvier) or homozygous mT/mG mice (Muzumdar et al., 2007) were used to produce SVZ primary cell cultures and for electroporation procedure as mentioned in the text. Cuprizone treatment (0.2% in food) started 5 weeks after electroporation and stopped 5 weeks later. Electroporation of post-natal animals was performed as described previously (Boutin et al., 2008) with minor modifications. In brief, pups were anesthetized by hypothermia and 2 μL of endotoxin-free plasmids (3 μg/μL for analyses in neonate and 6 μg/μL for young adult analyses in order to compensate for plasmid dilution) were injected into the left lateral ventricle. Electric pulses were applied immediately after DNA delivery (five pulses, 95 V, 50 ms pulse length, 950 ms intervals between two pulses) using a CUY21EDIT electroporator (Nepagene). Five or 7 weeks after electroporation, mT/mG mice were injected for 5 consecutive days with tamoxifen (180 mg/kg) to induce recombination and neuroblast labeling (this protocol was adopted based on preliminary tests, see Figures S3F and S3G).

Vector Constructions

Olig2 and *Sox10* sequences were amplified from mouse brain cDNA, using primers situated on either side of the coding sequence (Olig2-F: TTCGAGAGCTTAGATCATCC/Olig2-R: CCTTCT TGCAACAGAGCCC and Sox10-F: GACATGGCCGAGGAACA AG/Sox10-R: CCTCTAAGGTCGGGATAGA). Using the *Dcx* promoter of Dcx-Cre-iGFP plasmid (Franco et al., 2011), we designed and constructed six plasmids namely p*Dcx-Cre*, p*Dcx-Olig2*-IRES-*Cre*, p*Dcx-Sox10*-IRES-*Cre*, p*Dcx*-floxed*CreERT2*pA, p*Dcx*-floxed-*CreERT2*pA-*Olig2*, and p*Dcx*-floxed*CreERT2*pA-*Sox10* (Figure S1).

The specificity of our construction was first checked after *in vitro* transfection with the control plasmids (p*Dcx-Cre* and p*CMV*-stop-floxed-m*Gfp*): 2 days after SVZ cell transfection, all GFP$^+$ cells present in the culture were neuroblasts expressing DCX (Figure S3A) but negative for oligodendrocyte lineage marker OLIG2 (Figure S3B) and astrocyte marker (GFAP; Figure S3C) confirming that our strategy specifically drives transgene expression in neuroblasts.

SVZ Primary Cell Culture

Electroporated brains of 3-day-old CD1 mice were dissected out and sectioned into 400-μm-thick slices using a vibratome (Leica Microsysteme, Rueil Malmaison, France). SVZ was dissected in Hank's balanced salt solution. Dissection was performed in order to obtain solely SVZ tissue excluding all adjacent structures (white matter and striatum). Dissociated cells were cultured in defined medium as described (Chazal et al., 2000). The transfection by Magnetofection was only used to test the specificity of the DCX promoter. We used 3.5 μL of NeuroMag (OZ Biosciences, Marseille, France) for 1 μg of plasmids. DNA and NeuroMag were pre-incubated together for 20 min at room temperature, and then the cells were incubated with the mix for 20 min at 37°C on the magnetic plate to achieve transfection. Cells were analyzed for markers expression or morphometric analyses at various time points as indicated.

RNA Extraction and Real-Time RT-PCR

Total RNA and cDNA were prepared as described in El Waly et al. (2015). Real-time PCR reactions were performed in the Bio-Rad CFX96 real-time system (C1000 Thermal Cycler) using the SYBR GreenER qPCR SuperMix (Invitrogen, 1787623) with 2 μL of cDNA and 200 nM of each primer. Each reaction was performed in triplicate. Primers for the total transcripts of *Olig2* are: forward: agaccgagccaacaccag/reverse: aagctctcgaatgatccttcttt, the exogenous transcripts of *Olig2*: forward: gggctctgttgcaagaag/reverse located in plasmid: acatatagacaaacgcacacc, the total transcripts of *Sox10*: forward: atgtcagatgggaacccaga/reverse: gtctttggggtggttggag and the exogenous transcripts of *Sox10*: forward: tctatcccgacctta gagg/reverse located in plasmid: acatatagacaaacgcacacc.

Immunolabeling on Brain Sections and Cells

Mice were transcardially perfused with 4% paraformaldehyde. The brains were removed, post-fixed overnight, and cut into 50 μm coronal and sagittal sections using a vibratome (Leica Microsysteme, Rueil Malmaison, France). Immunofluorescent labeling was performed on sections or on cultured cells fixed with paraformaldehyde 4%. The following antibodies were used: anti-GFP (rabbit, 1/500; Life Technologies, A11122. Chicken, 1/500; Aves Labs GFP-1020), anti-DCX (goat, 1/100; Santa Cruz Sc-8066), anti-MBP (mouse IgG1, 1/500; Chemicon MAB384), anti-GFAP (mouse IgG 1/1,000; Sigma G3893), anti-OLIG2 (rabbit, 1/500; Chemicon AB 9610), anti-SOX9 (goat, 1/200; R&D AF3075), anti-PDGFRα (rat, 1/250; Chemicon CBL1366), anti-CC1 (mouse, 1/500; Calbiochem OP80), anti-CASPR/PARANODIN (rabbit, 1/500; L51, gift from Dr Goutebroze), anti-TCF4 (mouse IgG2a, 1/500; Millipore 05–511), anti-PSA-NCAM (mouse, $^1/_2$; supernatant produced in

our laboratory), anti-NEUROFILAMENT-160 (mouse, 1/500; Sigma N5264), and anti-βIV-SPECTRIN (mouse clone 393/2, 1/500; NeuroMab AB_2315816). The sections and cells were incubated with appropriate Alexa-conjugated secondary antibodies (1/500; Jackson ImmunoResearch Laboratories) then counterstained with Hoechst 33,342 (1/1,000; Sigma). Images were captured with a Zeiss apotome system (20× and 60× objectives) and a Zeiss 510 confocal (60× objective).

Morphometric Analysis

Morphometric analysis was performed using an automated and multithreaded Sholl for direct analysis of fluorescent images and traced morphologies using an ImageJ plugin. We used a series of concentric circles (15 μm) around the nucleus to calculate the number of branching intersections (Figure S2E). Cells where visualized using GFP for categories 1–3, DCX, and PDGFRα immunostaining for neuroblasts and OPCs, respectively. A minimum of 100 cells were analyzed for each experiment.

Electron Microscopy

Mice were perfused with 2.5% glutharaldehyde, 2% paraformaldehyde, and 0.1% tannic acid in PBS. Vibratome sections were obtained and incubated in uranyl acetate 1% in water overnight at 4°C and then dehydrated in ethanol and acetone before embedding in epon resin. Ultrathin sections of 90 nm were performed on a Leica Ultramicrotome (Leica, the Netherlands). For immunogold staining, ultrathin sections were incubated with saturated sodium metaperiodate for 2 min and incubated overnight at 4°C with rabbit anti-GFP after 1 hr blocking in 10% fetal calf serum. Samples were then incubated with secondary antibodies for 1 hr and fixed for 10 min in 2.5% glutharaldehyde in 0.05 M in cacodylate buffer. All Sections were counterstain with lead and micrographs were performed on a Tecnai G2 at 200 kV (FEI, the Netherlands). Micrographs were acquired with a Veleta camera (Olympus, Japan).

Quantification and Statistical Analysis

Cells were counted manually on pictures captured from confocal or apotome Zeiss microscope. The number of animals and cells counted for each analysis are synthesized on Table S1. All the presented values are means ± SEM unless otherwise stated. Data were statistically processed with non-parametric Mann-Whitney tests for independent two groups comparison or Wilcoxon test for paired two groups comparison. GFP^+ cells distribution in the brain was statistically processed with the chi-square test. qRT-PCR quantification on the endogenous and exogenous *Olig2* and *Sox10* were statistically processed with ANOVA and Kruskal-Wallis test. $p < 0.05$ was considered significant and $p < 0.01$ highly significant.

SUPPLEMENTAL INFORMATION

Supplemental Information includes five figures and one table and can be found with this article online at https://doi.org/10.1016/j.stemcr.2018.02.015.

AUTHOR CONTRIBUTIONS

B.E.W. conducted and designed the experiments and wrote the paper. M.C. and P.D. designed the experiments and wrote the paper.

ACKNOWLEDGMENTS

We are grateful to C. Maurange, L. Kerkerian-le Goff, and C. Bertet for critical reading of the manuscript. We also acknowledge the electron microscopy and microscopy platforms at the IBDM. This work was funded by CNRS, Aix-Marseille University, the Fondation pour la Recherche Médicale (DEC 20140329501), and the Fondation ARSEP. We also acknowledge France-bioimaging/PICSL infrastructure (ANR-10-INSB-04-01). B.E.W. was funded by FRM and ARSEP fellowship.

Received: December 4, 2017
Revised: February 26, 2018
Accepted: February 28, 2018
Published: March 29, 2018

REFERENCES

An, N., Xu, H., Gao, W.Q., and Yang, H. (2016). Direct conversion of somatic cells into induced neurons. Mol. Neurobiol. *55*, 642–651.

Boutin, C., Diestel, S., Desoeuvre, A., Tiveron, M.C., and Cremer, H. (2008). Efficient in vivo electroporation of the postnatal rodent forebrain. PLoS One *3*, e1883.

Braun, S.M., Pilz, G.A., Machado, R.A., Moss, J., Becher, B., Toni, N., and Jessberger, S. (2015). Programming hippocampal neural stem/progenitor cells into oligodendrocytes enhances remyelination in the adult brain after injury. Cell Rep. *11*, 1679–1685.

Brousse, B., Magalon, K., Durbec, P., and Cayre, M. (2015). Region and dynamic specificities of adult neural stem cells and oligodendrocyte precursors in myelin regeneration in the mouse brain. Biol. Open *4*, 980–992.

Cantarella, C., Cayre, M., Magalon, K., and Durbec, P. (2007). Intranasal HB-EGF administration favors adult SVZ cell mobilization to demyelinated lesions in mouse corpus callosum. Dev. Neurobiol. *68*, 223–236.

Capilla-Gonzalez, V., Cebrian-Silla, A., Guerrero-Cazares, H., Garcia-Verdugo, J.M., and Quinones-Hinojosa, A. (2013). The generation of oligodendroglial cells is preserved in the rostral migratory stream during aging. Front. Cell. Neurosci. *7*, 147.

Capilla-Gonzalez, V., Guerrero-Cazares, H., Bonsu, J.M., Gonzalez-Perez, O., Achanta, P., Wong, J., Garcia-Verdugo, J.M., and Quinones-Hinojosa, A. (2014). The subventricular zone is able to respond to a demyelinating lesion after localized radiation. Stem Cells *32*, 59–69.

Cayre, M., Bancila, M., Virard, I., Borges, A., and Durbec, P. (2006). Migrating and myelinating potential of subventricular zone neural progenitor cells in white matter tracts of the adult rodent brain. Mol. Cell. Neurosci. *31*, 748–758.

Cayre, M., Canoll, P., and Goldman, J.E. (2009). Cell migration in the normal and pathological postnatal mammalian brain. Prog. Neurobiol. *88*, 41–63.

Cayre, M., Courtes, S., Martineau, F., Giordano, M., Arnaud, K., Zamaron, A., and Durbec, P. (2013). Netrin 1 contributes to vascular remodeling in the subventricular zone and promotes

progenitor emigration after demyelination. Development *140*, 3107–3117.

Chazal, G., Durbec, P., Jankovski, A., Rougon, G., and Cremer, H. (2000). Consequences of neural cell adhesion molecule deficiency on cell migration in the rostral migratory stream of the mouse. J. Neurosci. *20*, 1446–1457.

Dai, J., Bercury, K.K., Ahrendsen, J.T., and Macklin, W.B. (2015). Olig1 function is required for oligodendrocyte differentiation in the mouse brain. J. Neurosci. *35*, 4386–4402.

El Waly, B., Buhler, E., Haddad, M.R., and Villard, L. (2015). Nhej1 deficiency causes abnormal development of the cerebral cortex. Mol. Neurobiol. *52*, 771–782.

El Waly, B., Macchi, M., Cayre, M., and Durbec, P. (2014). Oligodendrogenesis in the normal and pathological central nervous system. Front. Neurosci. *8*, 145.

Ernst, A., and Frisen, J. (2015). Adult neurogenesis in humans - common and unique traits in mammals. PLoS Biol. *13*, e1002045.

Franco, S.J., Martinez-Garay, I., Gil-Sanz, C., Harkins-Perry, S.R., and Muller, U. (2011). Reelin regulates cadherin function via Dab1/Rap1 to control neuronal migration and lamination in the neocortex. Neuron *69*, 482–497.

Franklin, R.J. (2002). Why does remyelination fail in multiple sclerosis? Nat. Rev. Neurosci. *3*, 705–714.

Franklin, R.J., Gilson, J.M., and Blakemore, W.F. (1997). Local recruitment of remyelinating cells in the repair of demyelination in the central nervous system. J. Neurosci. Res. *50*, 337–344.

Goings, G.E., Greisman, A., James, R.E., Abram, L.K., Begolka, W.S., Miller, S.D., and Szele, F.G. (2008). Hematopoietic cell activation in the subventricular zone after Theiler's virus infection. J. Neuroinflammation *5*, 44.

Heinrich, C., Bergami, M., Gascon, S., Lepier, A., Vigano, F., Dimou, L., Sutor, B., Berninger, B., and Gotz, M. (2014). Sox2-mediated conversion of NG2 glia into induced neurons in the injured adult cerebral cortex. Stem Cell Reports *3*, 1000–1014.

Jablonska, B., Aguirre, A., Raymond, M., Szabo, G., Kitabatake, Y., Sailor, K.A., Ming, G.L., Song, H., and Gallo, V. (2010). Chordin-induced lineage plasticity of adult SVZ neuroblasts after demyelination. Nat. Neurosci. *13*, 541–550.

Kim, J.B., Lee, H., Arauzo-Bravo, M.J., Hwang, K., Nam, D., Park, M.R., Zaehres, H., Park, K.I., and Lee, S.J. (2015). Oct4-induced oligodendrocyte progenitor cells enhance functional recovery in spinal cord injury model. EMBO J. *34*, 2971–2983.

Koizumi, H., Higginbotham, H., Poon, T., Tanaka, T., Brinkman, B.C., and Gleeson, J.G. (2006). Doublecortin maintains bipolar shape and nuclear translocation during migration in the adult forebrain. Nat. Neurosci. *9*, 779–786.

Kuspert, M., Hammer, A., Bosl, M.R., and Wegner, M. (2011). Olig2 regulates Sox10 expression in oligodendrocyte precursors through an evolutionary conserved distal enhancer. Nucleic Acids Res. *39*, 1280–1293.

Liu, Z., Hu, X., Cai, J., Liu, B., Peng, X., Wegner, M., and Qiu, M. (2007). Induction of oligodendrocyte differentiation by Olig2 and Sox10: evidence for reciprocal interactions and dosage-dependent mechanisms. Dev. Biol. *302*, 683–693.

Lois, C., and Alvarez-Buylla, A. (1994). Long-distance neuronal migration in the adult mammalian brain. Science *264*, 1145–1148.

Lois, C., Garcia-Verdugo, J.M., and Alvarez-Buylla, A. (1996). Chain migration of neuronal precursors. Science *271*, 978–981.

Lu, Q.R., Sun, T., Zhu, Z., Ma, N., Garcia, M., Stiles, C.D., and Rowitch, D.H. (2002). Common developmental requirement for Olig function indicates a motor neuron/oligodendrocyte connection. Cell *109*, 75–86.

Magalon, K., Cantarella, C., Monti, G., Cayre, M., and Durbec, P. (2007). Enriched environment promotes adult neural progenitor cell mobilization in mouse demyelination models. Eur. J. Neurosci. *25*, 761–771.

Marshall, C.A., Novitch, B.G., and Goldman, J.E. (2005). Olig2 directs astrocyte and oligodendrocyte formation in postnatal subventricular zone cells. J. Neurosci. *25*, 7289–7298.

Menn, B., Garcia-Verdugo, J.M., Yaschine, C., Gonzalez-Perez, O., Rowitch, D., and Alvarez-Buylla, A. (2006). Origin of oligodendrocytes in the subventricular zone of the adult brain. J. Neurosci. *26*, 7907–7918.

Mitew, S., Hay, C.M., Peckham, H., Xiao, J., Koenning, M., and Emery, B. (2014). Mechanisms regulating the development of oligodendrocytes and central nervous system myelin. Neuroscience *276*, 29–47.

Muzumdar, M.D., Tasic, B., Miyamichi, K., Li, L., and Luo, L. (2007). A global double-fluorescent Cre reporter mouse. Genesis *45*, 593–605.

Nait-Oumesmar, B., Decker, L., Lachapelle, F., Avellana-Adalid, V., Bachelin, C., and Van Evercooren, A.B. (1999). Progenitor cells of the adult mouse subventricular zone proliferate, migrate and differentiate into oligodendrocytes after demyelination. Eur. J. Neurosci. *11*, 4357–4366.

Nait-Oumesmar, B., Picard-Riera, N., Kerninon, C., Decker, L., Seilhean, D., Hoglinger, G.U., Hirsch, E.C., Reynolds, R., and Baron-Van Evercooren, A. (2007). Activation of the subventricular zone in multiple sclerosis: evidence for early glial progenitors. Proc. Natl. Acad. Sci. USA *104*, 4694–4699.

Najm, F.J., Lager, A.M., Zaremba, A., Wyatt, K., Caprariello, A.V., Factor, D.C., Karl, R.T., Maeda, T., Miller, R.H., and Tesar, P.J. (2013). Transcription factor-mediated reprogramming of fibroblasts to expandable, myelinogenic oligodendrocyte progenitor cells. Nat. Biotechnol. *31*, 426–433.

Picard-Riera, N., Decker, L., Delarasse, C., Goude, K., Nait-Oumesmar, B., Liblau, R., Pham-Dinh, D., and Evercooren, A.B. (2002). Experimental autoimmune encephalomyelitis mobilizes neural progenitors from the subventricular zone to undergo oligodendrogenesis in adult mice. Proc. Natl. Acad. Sci. USA *99*, 13211–13216.

Samanta, J., Grund, E.M., Silva, H.M., Lafaille, J.J., Fishell, G., and Salzer, J.L. (2015). Inhibition of Gli1 mobilizes endogenous neural stem cells for remyelination. Nature *526*, 448–452.

Stolt, C.C., Rehberg, S., Ader, M., Lommes, P., Riethmacher, D., Schachner, M., Bartsch, U., and Wegner, M. (2002). Terminal differentiation of myelin-forming oligodendrocytes depends on the transcription factor Sox10. Genes Dev. *16*, 165–170.

Suzuki, S.O., and Goldman, J.E. (2003). Multiple cell populations in the early postnatal subventricular zone take distinct migratory pathways: a dynamic study of glial and neuronal progenitor migration. J. Neurosci. *23*, 4240–4250.

Trapp, B.D., Nishiyama, A., Cheng, D., and Macklin, W. (1997). Differentiation and death of premyelinating oligodendrocytes in developing rodent brain. J. Cell Biol. *137*, 459–468.

Weider, M., Wegener, A., Schmitt, C., Kuspert, M., Hillgartner, S., Bosl, M.R., Hermans-Borgmeyer, I., Nait-Oumesmar, B., and Wegner, M. (2015). Elevated in vivo levels of a single transcription factor directly convert satellite glia into oligodendrocyte-like cells. PLoS Genet. *11*, e1005008.

Xing, Y.L., Roth, P.T., Stratton, J.A., Chuang, B.H., Danne, J., Ellis, S.L., Ng, S.W., Kilpatrick, T.J., and Merson, T.D. (2014). Adult neural precursor cells from the subventricular zone contribute significantly to oligodendrocyte regeneration and remyelination. J. Neurosci. *34*, 14128–14146.

Yang, N., Zuchero, J.B., Ahlenius, H., Marro, S., Ng, Y.H., Vierbuchen, T., Hawkins, J.S., Geissler, R., Barres, B.A., and Wernig, M. (2013). Generation of oligodendroglial cells by direct lineage conversion. Nat. Biotechnol. *31*, 434–439.

Zhou, Q., and Anderson, D.J. (2002). The bHLH transcription factors OLIG2 and OLIG1 couple neuronal and glial subtype specification. Cell *109*, 61–73.

Zhou, Q., Choi, G., and Anderson, D.J. (2001). The bHLH transcription factor Olig2 promotes oligodendrocyte differentiation in collaboration with Nkx2.2. Neuron *31*, 791–807.

Zhu, X., Zuo, H., Maher, B.J., Serwanski, D.R., LoTurco, J.J., Lu, Q.R., and Nishiyama, A. (2012). Olig2-dependent developmental fate switch of NG2 cells. Development *139*, 2299–2307.